

UDC 669.715 : 621.793.182

<https://doi.org/10.17073/0021-3438-2023-5-69-78>

Research article

Научная статья



Electron-ion-plasma surface modification of hypereutectic silumin

Yu.A. Shliarova¹, V.V. Shlyarov¹, D.V. Zaguliaev¹, Yu.F. Ivanov², V.E. Gromov¹¹ Siberian State Industrial University

42 Kirov Str., Novokuznetsk, 654007, Russia

² Institute of High-Current Electronics of Siberian Branch of the Russian Academy of Sciences

2/3 Akademicheskii Ave., Tomsk, 634055, Russia

✉ Yuliya A. Shliarova (rubannikova96@mail.ru)

Abstract: In this study, an integrated treatment approach was employed to modify hypereutectic silumin. This method involved electroexplosive alloying of the surface layer with yttrium oxide powder, followed by irradiation with a pulsed electron beam. The experimental data obtained demonstrate that this integrated treatment results in the formation of a submicron-nanocrystalline structure characterized by high-speed cellular crystallization of aluminum within the surface layer. This structure is composed of crystallization cells enriched with aluminum atoms, indicating the creation of a solid solution based on aluminum. The nanocrystalline layers, formed by silicon particles and yttrium oxide, are positioned at the cell boundaries. The study reveals that, as a consequence of integrated treatment with an electron beam energy density of 25 J/cm², the wear parameter of the modified samples increases by 7.9±0.6-fold, and the friction coefficient decreases by 1.7±0.15-fold compared to the initial state. Additionally, the microhardness of the modified silumin surface layer increases by 1.5±0.12-fold compared to the initial state. When the electron beam energy density is elevated to 35 J/cm², the wear parameter of silumin is enhanced by 2.1±0.21-fold, while the friction coefficient increases by 1.13±0.1-fold. However, the microhardness decreases by 1.3±0.13-fold, while still surpassing the specified characteristics of untreated silumin. This investigation postulates that the substantial increase in the wear parameter during integrated treatment may be attributed to the presence of silicon inclusions in the surface layer that did not dissolve during the modification process. These inclusions are surrounded by the high-speed cellular crystallization structure mentioned earlier.

Keywords: silumin, electroexplosive alloying, pulsed electron beam, structure, wear parameter.

Acknowledgments: This research was supported by the Russian Science Foundation, grant No. 19-79-10059,

<https://rscf.ru/project/19-79-10059/>

For citation: Shliarova Yu.A., Shlyarov V.V., Zaguliaev D.V., Ivanov Yu.F., Gromov V.E. Electron-ion-plasma surface modification of hypereutectic silumin. *Izvestiya. Non-Ferrous Metallurgy*. 2023;29(5):69–78. <https://doi.org/10.17073/0021-3438-2023-5-69-78>

Электронно-ионно-плазменное модифицирование поверхности силумина заэвтектического состава

Ю.А. Шлярова¹, В.В. Шляров¹, Д.В. Загуляев¹, Ю.Ф. Иванов², В.Е. Громов¹¹ Сибирский государственный индустриальный университет

654007, Россия, г. Новокузнецк, ул. Кирова, 42

² Институт сильноточной электроники СО РАН

634055, Россия, г. Томск, пр. Академический, 2/3

✉ Юлия Андреевна Шлярова (rubannikova96@mail.ru)

Аннотация: В настоящем исследовании проведена сложная обработка силумина заэвтектического состава, включающая комбинацию электровзрывного легирования поверхностного слоя порошком оксида иттрия с последующим облучением импульсным

электронным пучком. Полученные данные свидетельствуют о том, что такая комплексная обработка приводит к созданию многофазной субмикро-нанокристаллической структуры высокоскоростной ячеистой кристаллизации алюминия в поверхностном слое. Объем кристаллизационных ячеек обогащен атомами алюминия, что свидетельствует об образовании твердого раствора на основе алюминия. Нанокристаллические слои, образованные частицами кремния и оксидом иттрия, расположены вдоль границ ячеек. Исследование показывает, что в результате комплексной обработки при плотности энергии электронного пучка 25 Дж/см^2 происходит увеличение параметра износа модифицированных образцов в $7,9 \pm 0,6$ раза и уменьшение коэффициента трения в $1,7 \pm 0,15$ раза по сравнению с силумином в исходном состоянии. Кроме того, микротвердость модифицированного таким образом поверхностного слоя силумина возрастает по сравнению с исходным состоянием в $1,5 \pm 0,12$ раза. Повышение плотности энергии электронного пучка до 35 Дж/см^2 приводит к увеличению параметра износа силумина в $2,1 \pm 0,21$ раза, коэффициента трения в $1,13 \pm 0,1$ раза и снижению микротвердости в $1,3 \pm 0,13$ раза, при этом все еще превышая заданные характеристики силумина в исходном состоянии. В исследовании предполагается, что многократное увеличение параметра износа при комплексной обработке связано с присутствием в поверхностном слое включений кремния, которые не растворились при модификации, в окружении высокоскоростной ячеистой кристаллизационной структуры.

Ключевые слова: силумин, электровзрывное легирование, импульсный электронный пучок, структура, параметр износа.

Благодарности: Исследование выполнено за счет гранта Российского научного фонда № 19-79-10059, <https://rscf.ru/project/19-79-10059/>

Для цитирования: Шлярова Ю.А., Шляров В.В., Загуляев Д.В., Иванов Ю.Ф., Громов В.Е. Электронно-ионно-плазменное модифицирование поверхности силумина заэвтектического состава. *Известия вузов. Цветная металлургия*. 2023;29(5):69–78.

<https://doi.org/10.17073/0021-3438-2023-5-69-78>

Introduction

Hypereutectic aluminum-silicon (Al—Si) casting alloys find extensive applications in the aerospace, automotive, and general engineering industries. This popularity is primarily attributed to their excellent properties, including good castability, wear and corrosion resistance, high strength, low density, good thermal conductivity, and a low coefficient of thermal expansion. [1–3]. As a result, hypereutectic Al—Si alloys are becoming attractive materials to replace conventional cast iron in engineering applications such as cylinder blocks, cylinder liners, and pistons. This substitution aims to promote fuel economy and reduce vehicle gas emissions [4; 5].

The microstructure of hypereutectic Al—Si alloys typically includes primary Si crystals and an α -Al and eutectic Si mixture. As silicon content increases, primary silicon and elongated eutectic silicon can degrade the alloy's performance by disrupting the matrix. Therefore, modifying hypereutectic Al—Si alloys to alter the morphology and distribution of these silicon phases is vital for enhancing mechanical and tribological properties [6; 7]. Furthermore, it's well-established that exposing materials to intense pulsed electron beams leads to significant changes in their surface structure and properties [8–11]. The combination of beneficial features in intense pulsed electron beams is unquestionably the core for their use in advanced techniques for modifying metal materials.

In [12–14], the hypereutectic Al—17.5Si alloy underwent treatment with a high-current pulsed electron

beam. As a result, the treated surface exhibits different structural characteristics in various compositions and distribution zones: a silicon rich zone, an aluminum enriched zone, and an intermediate zone. The microstructure in the silicon-rich zone consists of small, dispersed, spherical nanosized Si crystals surrounded by Al cells. The aluminum-rich zone features a cellular microstructure with a cell size of $\sim 100 \text{ nm}$. The intermediate zone forms at the boundary between two zones and consists of a eutectic structure. As the number of pulses increases, the proportion of silicon-rich zone over the entire upper surface increases, and numerous cellular substructures transform into fine equiaxed grains. In a similar study [15], irradiation of hypereutectic silumin with a lower silicon content (Al—12.6Si) leads to the formation of a fine, equiaxed grain structure, significantly improving the wear resistance of the alloy (2.5-folds).

In [16], the surface alloying of an aluminum alloy with molybdenum using a high-current electron beam was investigated. As a result, it was discovered that after irradiation, an Al_5Mo phase with a needle-like structure appeared in the alloying layer. Numerous structural defects were observed, including craters, various cracks, dislocation loops, and dislocation walls. Studies of various irradiation modes have shown that with an increase in the number of pulses, the density and size of craters formed on the irradiated surface significantly decrease; and a noticeable increase in corrosion resistance is also observed. An international scientific team conducted

research on the influence of electron beam treatment on the solubility of Sc in Al and the associated hardening effects [17].

The high-current pulsed electron beam treatment of hypereutectic Al–15Si alloy increases the tensile strength of the alloy by 41.4 %. This treatment method appears to be a good approach for enhancing the mechanical properties of hypereutectic alloys within the Al–Si system [18].

One of the most promising techniques for surface treatment of metals and alloys is the electron-ion-plasma method, which involves both coating and subsequent irradiation with an electron beam. This combination of methods enables not only the application of thermal effects to the material's surface but also alloying of the surface layer [19–21]. Collectively, these methods for influencing the structure and phase composition offer the potential to mitigate many of the shortcomings and extend the service life of machine parts and mechanisms.

The aim of this study is to investigate and analyze the patterns governing the formation of the structure and properties of hypereutectic silumin when subjected to modification with yttrium oxide particles using an integrated method that combines electroexplosive alloying with subsequent irradiation via a pulsed electron beam.

Materials and methods

In order to conduct this study at Siberian State Industrial University (SibSIU, Novokuznetsk), we produced five samples of silumin with a eutectic composition, comprising the following elements: Si — 20.28 wt.%, Fe — 1.14 %, Cu — 0.072 %, Mn — 0.015 %, Ni — 0.006 %, Ti — 0.006 %, Cr — 0.001 %, with the remainder being aluminum.

The first step of treatment involved electroexplosive alloying of the silumin. This process was carried out using an EVU 60/10 electric discharge unit at SibSIU. Aluminum foil served as the material for the exploding conductors, while Y_2O_3 was employed as the powder sample. The treatment was conducted under the following conditions: aluminum foil weight — 58.9 mg, Y_2O_3 powder mass — 58.9 mg, discharge voltage — 2.8 kV.

In the second stage, the modified surface of silumin samples underwent irradiation with a pulsed electron beam. The irradiation was performed using the SOLO facility (Institute of High Current Electronics, SB RAS, Tomsk). The irradiation parameters were as follows: accelerated electron energy — 18 keV, electron beam ener-

gy density — 25 and 35 J/cm², electron beam pulse duration — 150 μ s, number of current pulses — 3, and pulse repetition rate — 0.3 s^{–1}.

The analysis of the irradiated surface's structure was conducted using scanning electron microscopy with an SEM-515 device (Philips, Netherlands). The elemental composition of the material's surface layer was determined through X-ray spectral microanalysis using an EDAX ECON IV microanalyzer, an attachment to the SEM-515 scanning electron microscope (Philips, Germany). The structural-phase state of the silumin, depending on the distance to the modification surface, was investigated using transmission electron diffraction microscopy of thin foils with a JEM-2100F device (JEOL, Japan). This technique enabled the study of defect substructures, phase composition, and highly sensitive scanning with an electron beam, as well as the examination of the foil's elemental composition through energy dispersive analysis of X-ray radiation. The mechanical properties of modified silumin were assessed at room temperature in air, including microhardness determination using a PMT-3 device (JSC LOMO, St. Petersburg) with an indenter load of 0.5 N. The tribological properties of the modified silumin were characterized using a TRIBOTester device, employing the Pin-on-Disc test method (France). These tests were conducted at room temperature in air, with an Al_2O_3 ball (diameter: 6 mm) as the indenter, a 5 N load on the indenter, a sample rotation speed of 25 mm/s, and a friction path length of 100 m.

Results and discussion

The studies conducted included the irradiation of silumin samples doped using the electroexplosive method. The samples were exposed to a pulsed electron beam with an energy density of 25 J/cm². A significant reduction in the wear parameter of the modified samples by 7.9 ± 0.6 -fold and the friction coefficient by 1.7 ± 0.15 -fold was observed compared to the cast silumin in its original state. The microhardness of the surface layer of the silumin modified in this manner showed a relatively small increase: 1.5 ± 0.12 -fold. However, an increase in the energy density of the electron beam to 35 J/cm² resulted in a 2.1 ± 0.21 -fold increase in the silumin wear parameter and a 1.13 ± 0.1 -fold increase in the friction coefficient. Additionally, there was a 1.3 ± 0.13 -fold decrease in microhardness compared to the characteristics of silumin modified at an electron beam energy density of 25 J/cm² while still exceeding the characteristics of the original silumin state.

It is evident that the mechanical and tribological characteristics of silumin are determined by the state of the structure of the modified surface layer. Figure 1 displays electron microscopic images of the silumin surface structure in its initial state, illustrating the presence of numerous faceted inclusions (dark-colored particles), needle-shaped inclusions, and inclusions resembling Chinese hieroglyphs.

It is widely recognized that faceted inclusions are silicon particles (the dark-colored particles), while hieroglyphic inclusions and needle inclusions consist of complex compounds (the light-colored particles) formed by aluminum, iron, copper, manganese, and silicon atoms [22].

In a previous study [23], focusing on silumins with eutectic composition, it was demonstrated that integrated treatment combining electroexplosive alloying with yttrium oxide and subsequent irradiation with a pulsed electron beam (at 40 J/cm^2 , $200 \text{ }\mu\text{s}$ pulse duration, and 3 pulses) results in the formation of a surface layer up to $150 \text{ }\mu\text{m}$ thick. This layer exhibits a high-speed cellular crystallization structure, with cell volumes ranging between $400\text{--}800 \text{ nm}$ and being comprised of an aluminum-based solid solution. These cells are separated by interlayers up to 100 nm thick, which are composed of silicon and intermetallic compounds with complex elemental compositions. This observed modification of silumin leads to a 3.5-fold increase in wear resistance, a 1.3-fold decrease in the coefficient of friction, and a 1.2-fold increase in microhardness compared to the original material. It can be hypothesized that the patterns of structural and property evolution previously established for silumin of eutectic composition, as described in [19], will al-

so be observed in silumin with a hypereutectic composition. Indeed, the studies conducted in this work revealed the formation of a high-speed cellular crystallization structure during integrated treatment of hypereutectic silumin (Fig. 2).

X-ray microanalysis of the foils, as shown in Fig. 3, revealed that the cell volume is enriched with aluminum atoms, while the interlayers situated along the cell boundaries are predominantly enriched with silicon and yttrium atoms. Additionally, atoms of oxygen, iron, titanium, and nickel were detected in small quantities within the studied layer. These elements are considered impurities in the material under investigation.

A distinctive feature of the structure of hypereutectic silumin, which has undergone integrated modification, is the presence of silicon inclusions in the surface layer that did not dissolve during high-energy treatment. When the surface modified by the electroexplosive method is irradiated with a pulsed electron beam at an electron beam energy density of 25 J/cm^2 , it results in the formation of a microtwin structure within the silicon inclusions (Fig. 4, *a*, *c*). At the same time, the silicon inclusions themselves maintain their faceted shape, which is characteristic of inclusions in cast silumin. As depicted in Fig. 4, there is evidence of the formation of silumin layers situated along the boundaries of aluminum crystallization cells. These layers exhibit a nanocrystalline structure with grains measuring $10\text{--}15 \text{ nm}$ (Fig. 4, *c*). Additionally, the presence of yttrium oxysilicide particles is observed (Fig. 4, *d*).

Irradiating silumin with a pulsed electron beam at an electron beam energy density of 35 J/cm^2 results in

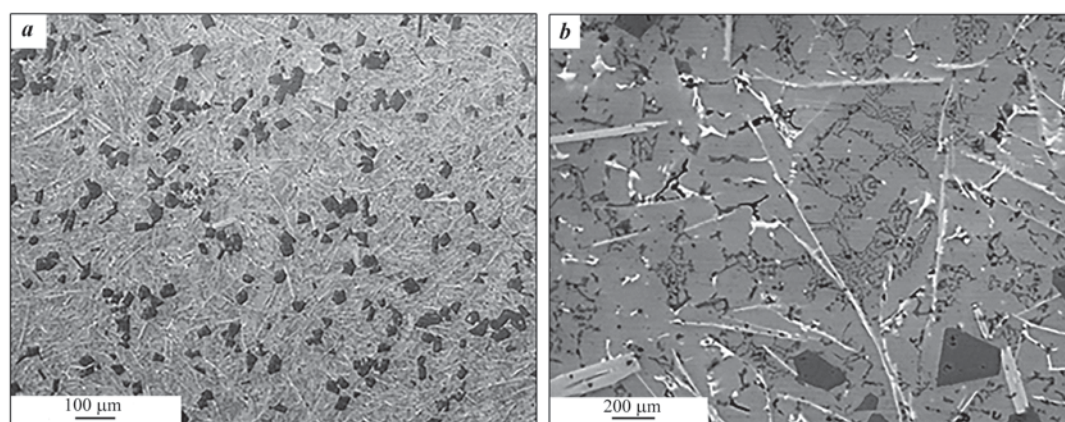


Fig. 1. Electron microscopic images of the structure of hypereutectic silumin in the initial state

Рис. 1. Электронно-микроскопические изображения структуры силумина заэвтектического состава в исходном состоянии

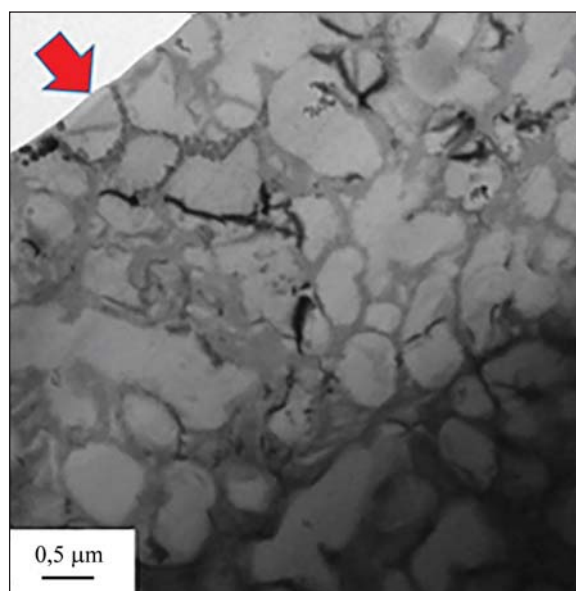


Fig. 2. Electron microscopic image of the structure of high-speed cellular crystallization formed in the surface layer of hypereutectic silumin exposed to electroexplosive alloying by yttrium oxide and subsequent irradiation by pulsed electron beam at an electron beam density of 25 J/cm^2

Modified surface is indicated by an arrow

Рис. 2. Электронно-микроскопическое изображение структуры высокоскоростной ячеистой кристаллизации, формирующейся в поверхностном слое силумина заэвтектического состава, подвергнутого электровзрывному легированию оксидом иттрия и последующему облучению импульсным электронным пучком при плотности энергии пучка электронов 25 Дж/см^2

Стрелкой указана поверхность модифицирования

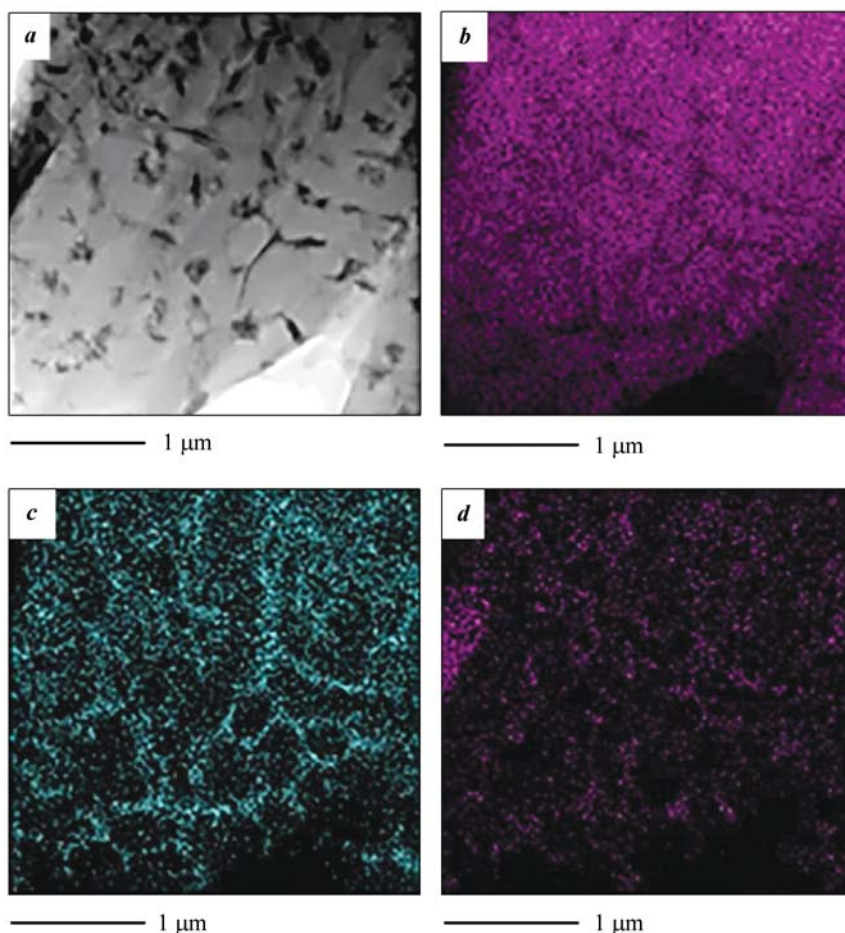


Fig. 3. Electron microscopic image of the structure of the silumin surface layer exposed to integrated treatment (25 J/cm^2) (a), and images of foil segment a, acquired in characteristic X-ray irradiation of aluminum (b), silicon (c), and yttrium (d) atoms

Рис. 3. Электронно-микроскопическое изображение структуры поверхностного слоя силумина, подвергнутого комплексной обработке (25 Дж/см^2) (a), и изображения участка фольги a, полученные в характеристическом рентгеновском излучении атомов алюминия (b), кремния (c), иттрия (d)

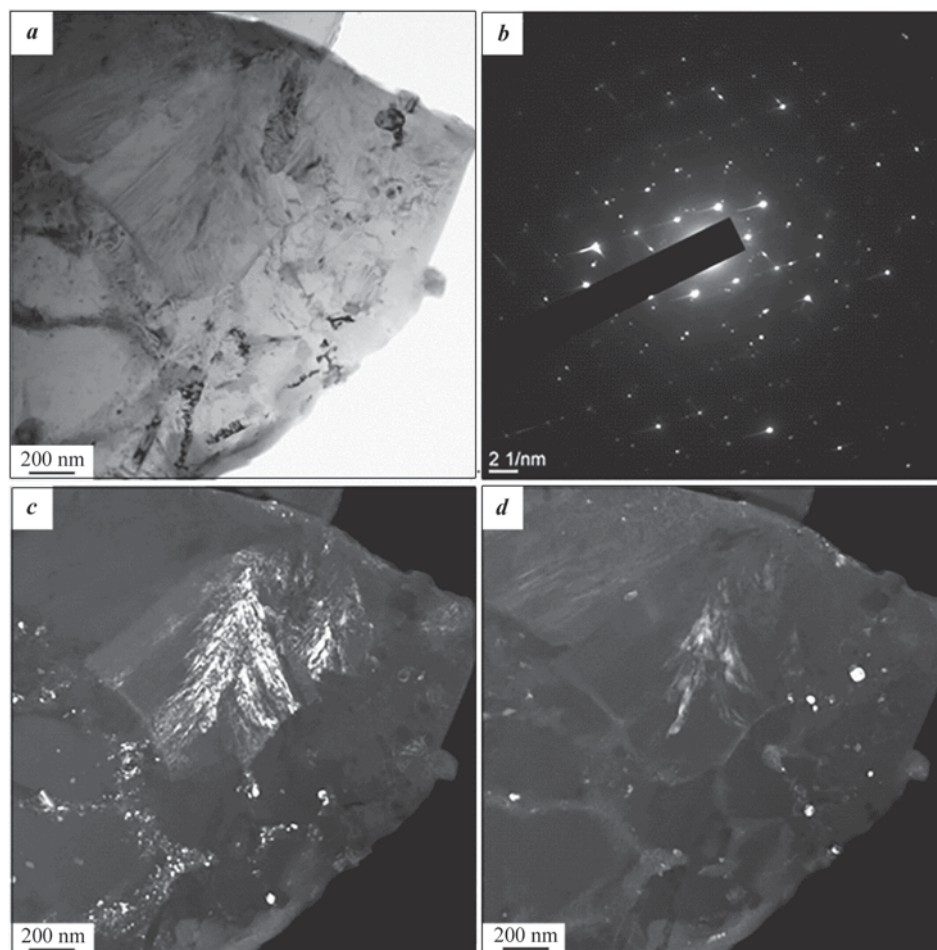


Fig. 4. Electron microscopic image of structure formed in the surface layer of hypereutectic silumin exposed to electroexplosive alloying by yttrium oxide and subsequent irradiation by pulsed electron beam at an electron beam energy density of 25 J/cm^2

a – light filed; *b* – electron diffraction pattern; *c, d* – dark fields acquired in reflections $[111] \text{ Si}$ (*c*) and $[022] \text{ Y}_2\text{SiO}_5$ (*d*)

Рис. 4. Электронно-микроскопическое изображение структуры, формирующейся в поверхностном слое силумина заэвтектического состава, подвергнутого электровзрывному легированию оксидом иттрия и последующему облучению импульсным электронным пучком при плотности энергии пучка электронов 25 Дж/см^2
a – светлое поле; *b* – микроэлектронограмма; *c, d* – темные поля, полученные в рефlekсах $[111] \text{ Si}$ (*c*) и $[022] \text{ Y}_2\text{SiO}_5$ (*d*)

the development of a nanocrystalline structure within the preserved silicon inclusions, with the grains measuring between 9–30 nm. Notably, these inclusions assume a rounded (globular) shape (Fig. 5). Similar to the scenario illustrated in Fig. 4, the partial dissolution of silicon inclusions followed by high-speed crystallization of the surface layer leads to the formation of a cellular structure. This structure is characterized by the precipitation of nanosized silicon particles and yttrium oxysilicides along the boundaries of the cells (Fig. 5, *c, d*).

The collection of results obtained leads us to infer that the significant enhancement in the wear resistance of silumin, following integrated treatment, can

be attributed, at least in part, to the presence of silicon inclusions that did not dissolve during modification, surrounded by a structure of high-speed cellular crystallization in the surface layer. These inclusions are surrounded by a high-speed cellular crystallization structure in the surface layer. This effect is observed not only in comparison to the untreated cast silumin but also in comparison to eutectic silumin that underwent a similar modification process.

Conclusions

1. Integrated treatment, which combines electroexplosive alloying with subsequent pulse irradiation

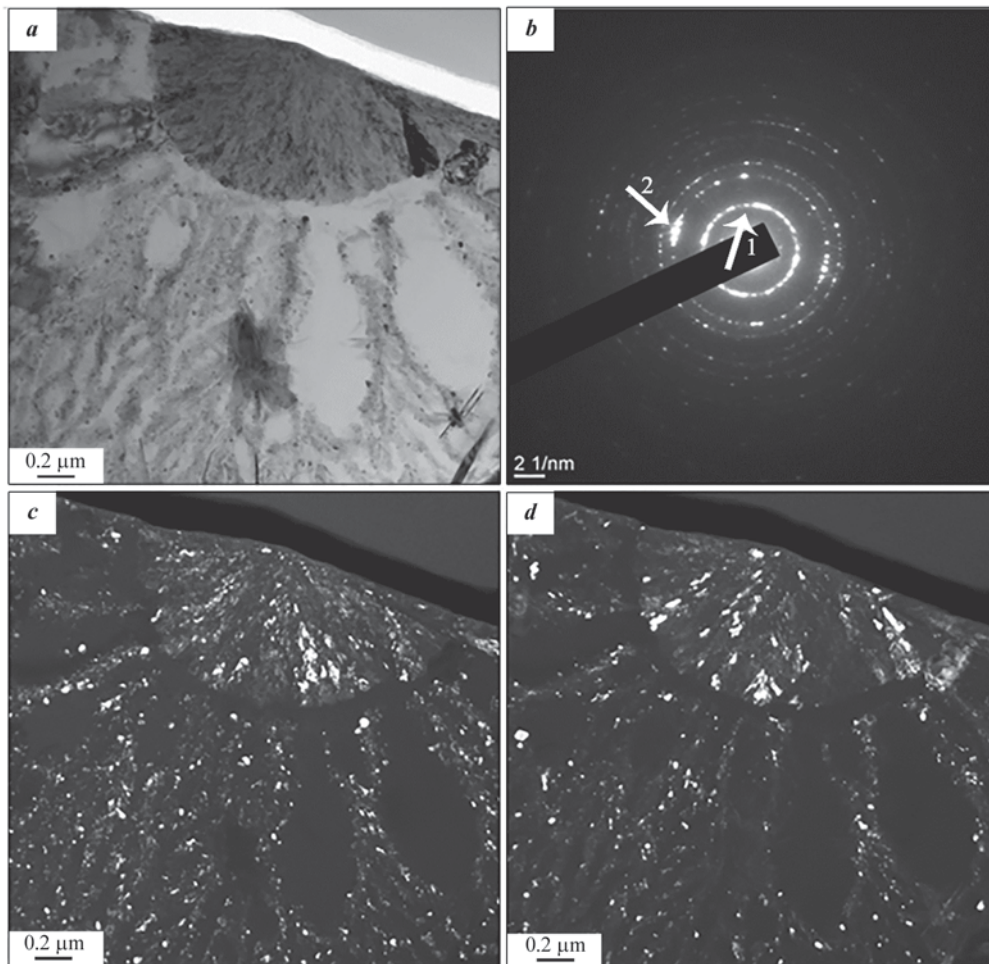


Fig. 5. Electron microscopic image of the structure formed in the surface layer of hypereutectic silumin exposed to electroexplosive alloying by yttrium oxide and subsequent irradiation by pulsed electron beam at an electron beam energy density of 35 J/cm^2

a – light filed; *b* – electron diffraction pattern;

c, d – dark fields acquired in reflections $[111] \text{ Si}$ (*c*) and $[032] \text{ Y}_2\text{Si}_2\text{O}_7$ (*d*)

Рис. 5. Электронно-микроскопическое изображение структуры, формирующейся в поверхностном слое силумина заэвтектического состава, подвергнутого электровзрывному легированию оксидом иттрия

и последующему облучению импульсным электронным пучком при плотности энергии пучка электронов 35 Дж/см^2

a – светлое поле; *b* – микроэлектроннограмма; *c, d* – темные поля, полученные в рефlekсах

1 – $[111] \text{ Si}$ (*c*) и *2* – $[220] \text{ Si} + [032] \text{ Y}_2\text{Si}_2\text{O}_7$ (*d*)

tion using an electron beam at an energy density of 25 J/cm^2 , results in a substantial 7.9 ± 0.6 -fold increase in wear parameter of the modified samples and a 1.7 ± 0.15 -fold reduction in the friction coefficient compared to the initial state of the silumin. Additionally, the microhardness of the silumin surface layer increases by 1.5 ± 0.12 -fold relative to its initial state.

2. Irradiation of samples with an electron beam energy density of 35 J/cm^2 leads to a 2.1 ± 0.21 -fold increase in the silumin wear parameter and a 1.13 ± 0.1 -fold increase in the friction coefficient, along

with a 1.3 ± 0.13 -fold decrease in microhardness compared to samples modified at an electron beam energy density of 25 J/cm^2 .

3. It is postulated that the substantial increase in the wear parameter of silumin following integrated treatment, when compared to both the untreated cast silumin and eutectic silumin modified in a similar manner, can be attributed to the presence of silicon inclusions in the surface layer. These silicon inclusions, which remained intact during modification, are surrounded by a high-speed cellular crystallization structure.

References

1. Tutunchilar S., Besharati Givi M.K., Haghpanahi M., Asadi P. Eutectic Al—Si piston alloy surface transformed to modified hypereutectic alloy via FSP. *Materials Science and Engineering: A*. 2012;534:557–567.
<https://doi.org/10.1016/j.msea.2011.12.008>
2. Mohamed A.M.A., Samuel A.M., Samuel F.H., Doty H.W. Influence of additives on the microstructure and tensile properties of near-eutectic Al—10.8%Si cast alloy. *Materials & Design*. 2009;30(10):3943–3957.
<https://doi.org/10.1016/j.matdes.2009.05.042>
3. Li Q., Xia T., Lan Y., Li P., Fan L. Effects of rare earth Er addition on microstructure and mechanical properties of hypereutectic Al—20% Si alloy. *Materials Science and Engineering: A*. 2013;588:97–102.
<https://doi.org/10.1016/j.msea.2013.09.017>
4. Chen M., Meng-Burany X., Perry T.A., Alpas A.T. Micromechanisms and mechanics of ultra-mild wear in Al—Si alloys. *Acta Materialia*. 2008;56(19):5605–5616.
<https://doi.org/10.1016/j.actamat.2008.07.043>
5. Chen M., Alpas A.T. Ultra-mild wear of a hypereutectic Al—18.5wt.%Si alloy. *Wear*. 2008;265(1-2):186–195.
<https://doi.org/10.1016/j.wear.2007.10.002>
6. Cao F., Jia Y., Prashanth K.G., Ma P., Liu J., Scudino S., Huang F., Eckert J., Sun J. Evolution of microstructure and mechanical properties of as-cast Al—50Si alloy due to heat treatment and P modifier content. *Materials & Design*. 2015;74:150–156.
<https://doi.org/10.1016/j.matdes.2015.03.008>
7. Li Q., Xia T., Lan Y., Zhao W., Fan L., Li P. Effect of in situ γ -Al₂O₃ particles on the microstructure of hypereutectic Al—20%Si alloy. *Journal of Alloys and Compounds*. 2013;577:232–236.
<https://doi.org/10.1016/j.jallcom.2013.04.043>
8. Wenhai P., Shengzhi H., Jun C., Wei L., Limin Z., Jun D. Surface composite microstructure and improved mechanical property of YG10X cemented carbide induced by high current pulsed electron beam irradiation. *International Journal of Refractory Metals and Hard Materials*. 2019;78:233–239.
<https://doi.org/10.1016/j.ijrmhm.2018.09.016>
9. Hangyu Y., Yuyong C., Xiaopeng W., Fantao K. Effect of beam current on microstructure, phase, grain characteristic and mechanical properties of Ti—47Al—2Cr—2Nb alloy fabricated by selective electron beam melting. *Journal of Alloys and Compounds*. 2018;750:617–625.
<https://doi.org/10.1016/j.jallcom.2018.03.343>
10. Wei J., Langping W., Xiaofeng W. Studies on surface topography and mechanical properties of TiN coating irradiated by high current pulsed electron beam. *Nuclear Instruments and Methods in Physics Research Section B: Beam Interactions with Materials and Atoms*. 2018;436:63–67.
<https://doi.org/10.1016/j.nimb.2018.09.003>
11. Zou J., Qin Y., Dong C., Wang X., Almin W., Hao S. Numerical simulation of the thermal-mechanical process of high current pulsed electron beam treatment. *Journal of Vacuum Science and Technology A: Vacuum, Surfaces and Films*. 2004;22(3):545–552.
<https://doi.org/10.1116/1.1697481>
12. Gao B., Hao Y., Zhuang W.F., Tu G.F., Shi W.X., Li S.W., Hao S.Z., Dong C., Li M.C. Study on continuous solid solution of Al and Si elements of a high current pulsed electron beam treated hypereutectic Al—17.5Si alloy. *Physics Procedia*. 2011;18:187–192.
<https://doi.org/10.1016/j.phpro.2011.06.079>
13. Gao B., Hu L., Li S., Hao Y., Zhang Y., Tu G., Grosdidier T. Study on the nanostructure formation mechanism of hypereutectic Al—17.5Si alloy induced by high current pulsed electron beam. *Applied Surface Science*. 2015;346:147–157.
<https://doi.org/10.1016/j.apsusc.2015.04.029>
14. Hu L., Gao B., Lv J.K., Hao Y., Tu G.F., Hao S.Z., Dong C. The metastable structure of hypereutectic Al—17.5Si alloy surface induced by high current pulsed electron beam. *Materials Research Innovations*. 2015;19:S5320–S5324.
<https://doi.org/10.1179/1432891714Z.0000000001102>
15. Hao Y., Gao B., Tu G.F., Cao H., Hao S.Z., Dong C. Surface modification of Al—12.6Si alloy by high current pulsed electron beam. *Applied Surface Science*. 2012;258:2052–2056.
<https://doi.org/10.1016/j.apsusc.2011.04.104>
16. Xia H., Zhang C., Lv P., Cai J., Jin Y., Guan Q. Surface alloying of aluminum with molybdenum by high-current pulsed electron beam. *Nuclear Instruments and Methods in Physics Research Section B: Beam Interactions with Materials and Atoms*. 2018;416:9–15.
<https://doi.org/10.1016/j.nimb.2017.11.028>
17. Tomus D., Qian M., Brice C.A., Muddle B.C. Electron beam processing of Al—2Sc alloy for enhanced precipitation hardening. *Scripta Materialia*. 2010;63(2):151–154.
<https://doi.org/10.1016/j.scriptamat.2010.03.039>
18. Bo G., Ning X., Pengfei X. Shock wave induced

- nanocrystallization during the high current pulsed electron beam process and its effect on mechanical properties. *Materials Letters*. 2019;237:180–184.
<https://doi.org/10.1016/j.matlet.2018.11.054>
19. Zaguliaev D., Gromov V., Rubannikova Yu., Kononov S., Ivanov Yu., Romanov D., Semin A. Structure and phase states modification of Al–11Si–2Cu alloy processed by ion-plasma jet and pulsed electron beam. *Surface and Coatings Technology*. 2020; 383:125246.
<https://doi.org/10.1016/j.surfcoat.2019.125246>
 20. Zaguliaev D., Kononov S., Ivanov Yu., Gromov V., Petrikova E. Microstructure and mechanical properties of doped and electron-beam treated surface of hypereutectic Al–11.1%Si alloy. *Journal of Materials Research and Technology*. 2019;8(5):3835–3842.
<https://doi.org/10.1016/j.jmrt.2019.06.045>
 21. Zaguliaev D., Kononov S., Ivanov Yu., Gromov V. Effect of electron-plasma alloying on structure and mechanical properties of Al–Si alloy. *Applied Surface Science*. 2019;498:143767.
<https://doi.org/10.1016/j.apsusc.2019.143767>
 22. Belov N.A., Savchenko S.V., Khvan A.V. Phase composition and structure of silumins. Moscow: MISIS, 2008. 282 p. (In Russ.).
Белов Н.А., Савченко С.В., Хван А.В. Фазовый состав и структура силуминов. М.: МИСиС, 2008. 282 с.
 23. Gromov V.E., Zagulyaev D.V., Ivanov Yu.F., Kononov S.V., Nevskii S.A., Sarychev V.D., Budovskikh E.A., Rubannikova Yu.A. Structure and hardening of silumin modified by electron-ion plasma. Novokuznetsk: Publishing Center SibGIU, 2020. 284 p. (In Russ.).
Громов В.Е., Загуляев Д.В., Иванов Ю.Ф., Коновалов С.В., Невский С.А., Сарычев В.Д., Будовских Е.А., Рубанникова Ю.А. Структура и упрочнение силумина, модифицированного электронно-ионной плазмой. Новокузнецк: Изд центр СибГИУ, 2020. 284 с.

Information about the authors

Yuliya A. Shliarova – Postgraduate Student of the Department of Natural Science Disciplines of Siberian State Industrial University (SibSIU), Researcher of the Laboratory of electron microscopy and image processing of SibSIU.
<https://orcid.org/0000-0001-5677-1427>
E-mail: rubannikova96@mail.ru

Vitaliy V. Shlyarov – Postgraduate Student of SibSIU, Researcher of the Laboratory of electron microscopy and image processing of SibSIU.
<https://orcid.org/0000-0001-8130-648X>
E-mail: shlyarov@mail.ru

Dmitriy V. Zaguliaev – Dr. Sci. (Eng.). Deputy Head of Scientific Research Department of SibSIU.
<https://orcid.org/0000-0002-9859-8949>
E-mail: zagulyaev_dv@physics.sibsiu.ru

Yuriy F. Ivanov – Dr. Sci. (Phys.-Math.), Professor, Chief Researcher of the Institute of High-Current Electronics of Siberian Branch of the Russian Academy of Sciences.
<https://orcid.org/0000-0001-8022-7958>
E-mail: yufi55@mail.ru

Viktor E. Gromov – Dr. Sci. (Phys.-Math.), Professor, Head of the Department of Natural Science Disciplines of SibSIU.
<https://orcid.org/0000-0002-5147-5343>
E-mail: gromov@physics.sibsiu.ru

Информация об авторах

Юлия Андреевна Шлярова – аспирант кафедры естественно-научных дисциплин Сибирского государственного индустриального университета (СибГИУ), научный сотрудник лаборатории электронной микроскопии и обработки изображений СибГИУ.
<https://orcid.org/0000-0001-5677-1427>
E-mail: rubannikova96@mail.ru

Виталий Владиславович Шляров – аспирант кафедры естественно-научных дисциплин СибГИУ, научный сотрудник лаборатории электронной микроскопии и обработки изображений СибГИУ.
<https://orcid.org/0000-0001-8130-648X>
E-mail: shlyarov@mail.ru

Дмитрий Валерьевич Загуляев – д.т.н., зам. начальника управления научных исследований СибГИУ.
<https://orcid.org/0000-0002-9859-8949>
E-mail: zagulyaev_dv@physics.sibsiu.ru

Юрий Федорович Иванов – д.ф.-м.н., профессор, главный научный сотрудник Института сильноточной электроники СО РАН.
<https://orcid.org/0000-0001-8022-7958>
E-mail: yufi55@mail.ru

Виктор Евгеньевич Громов – д.ф.-м.н., профессор, заведующий кафедрой естественно-научных дисциплин СибГИУ.
<https://orcid.org/0000-0002-5147-5343>
E-mail: gromov@physics.sibsiu.ru

Contribution of the authors

Yu.A. Shliarova – formulation of the main concept, goal, and objectives of the study, manuscript writing.

V.V. Shlyarov – experiment preparation, experiment execution, literature review.

D.V. Zaguliaev – scientific guidance, manuscript revision, and results analysis.

Yu.F. Ivanov – electron microscopic studies, results analysis.

V.E. Gromov – work concept, TEM images analysis, manuscript writing, conclusions formulation.

Вклад авторов

Ю.А. Шлярова – формирование основной концепции, постановка цели и задачи исследования, подготовка текста.

В.В. Шляров – подготовка экспериментов, проведение экспериментов, обзор литературы.

Д.В. Загуляев – научное руководство, корректировка текста, корректировка выводов.

Ю.Ф. Иванов – проведение электронно-микроскопических исследований, анализ результатов.

В.Е. Громов – концепция работы, анализ ПЭМ-изображений, подготовка текста, формулировка выводов.

The article was submitted 03.02.2023, revised 25.05.2023, accepted for publication 30.05.2023

Статья поступила в редакцию 03.02.2023, доработана 25.05.2023, подписана в печать 30.05.2023